Journal of Scientific Enquiry
Research Article
Vol: 1, Pages: 38-43

A facile synthesis of highly crystalline ZnO nanoparticles via green synthesis route using *Moringa oleifera* leaf extract at relatively low temperature

Tatan Ghosh[a*], **Subhamay Pramanik**[b], **Probodh K. Kuiri**[b]

[a] *Department of Physics, Balarampur College, P.O.-Rangadih, Purulia – 723143, West Bengal, India*
[b] *Department of Physics, Sidho-Kanho-Birsha University, Purulia – 723104, West Bengal, India*

Received: 05.10.2021; accepted: 22.10.2021; published online: 30.12.2021

In this work we report a facile synthesis method for preparation of zinc oxide (ZnO) nanoparticles (NPs) using Moringa oleifera leaf extract at relatively low temperature. We have synthesized highly crystalline ZnO NPs of average size 45 ± 6 nm through a very simplistic technique. Any extra chemicals and high temperature has not been employed to formulate the synthesis process a cost effective and energy efficient in a sustainable and eco-friendly way. Various basic and comprehensive characterization techniques like X-ray diffraction study, scanning electron microscopy, energy-dispersive X-ray spectroscopy, optical absorption spectroscopy, photoluminescence spectroscopy and Fourier transformed infrared spectroscopy has been used for structural and optical studies of the synthesized samples. The large scale production and medical application of the prepared sample can be feasible as it is produced via green synthesis approach following the principle of green chemistry.

Key words: ZnO nanoparticles, green synthesis, *Moringa oleifera* leaf extract, characterization of nanoparticles

1. Introduction

Recently metal oxide nanoparticles (NPs) of various transition metals like Zn, Cu, Ti and Fe have been paid enormous attention by the scientific community due to their vast application in different areas like biomedical, catalysis, solar cells, cosmetics, sensors, etc. [1–4]. Among these, ZnO NPs have received significant attention not only due to its cost effectiveness but also high chemical stability, efficient biocompatibility, high photocatalytic activity, etc. ZnO NPs have widely been used in solar cells, cosmetics, optical devices, catalysts, textile industry, different medical applications including carrier and delivery of drug, bioimaging and many others. They also exhibit high photocatalytic activity and efficient antimicrobial efficiency over a wide spectrum of microorganisms [5].

An enumerable number of synthesis methods have been employed for synthesis of ZnO NPs some of which includes ball milling[6], ion beam implantation [7], thermal decomposition [8], solvothermal [9], hydrothermal [10], solgel [11] co-precipitation methods [12–13]. Although these methods are very efficient for synthesis of ZnO NPs but using biological components instead of using hazard chemicals has always been a suitable choice towards an environment friendly approach. Additionally, the better control of size and shape of the NPs can be obtained [14]. In our previous studies we have successfully control the size of green synthesized Ag NPs by varying the leaf extract of Neem [15] and Guava [16] plant in a fixed concentration of silver nitrate solution at room temperature. Various plant extracts has been used for synthesizing ZnO NPs in green synthesis route [17]. Using *Moringa Oleifera* leaves extract for preparation of green synthesized ZnO NPs has also been achieved by many research groups [18, 19].

In this work, we have synthesized ZnO NPs at comparatively low temperature ($\sim 70\,^{\circ}$C) in green synthesis route using *Moringa Oleifera* leaf extract. Here no extra chemicals apart from precursor (Zinc acetate dihydrate) and precipitator (Potassium hydroxide) have been employed obeying strictly the principle of green chemistry. For optical characterization of the sample we have used UV-Visible spectroscopy, photoluminescence (PL) spectroscopy and Fourier-transform-infrared (FTIR) spectroscopy; for structural study X-ray diffraction (XRD), scanning electron microscopy (SEM) and for elemental analysis energy-dispersive X-ray spectroscopy (EDS) have been used.

2. Experimental Details and Characterization Techniques

Here we have used green synthesis method where *Moringa Oleifera* (Drumstick) leaves extract has

*Email for correspondence-tatanghosh83@gmail.com

 DOI: https://doi.org/10.54280/21/03

been used as a natural reducing and capping agent. *Moringa Oleifera* tree belongs to the single genus in the Moringaceae family. It is a fast-growing tree spread widely in Africa and Asia. The leaf, flower and pods of this tree are used as vegetables. The different parts of this plant has been served as folk medicine since long past [20]. Drumstick leaves contains a rich source of vitamins like L-ascorbic acid, retinol, niacin; flavanoids like quercetin, kaempferol, myricetin, isorhamnetin; phenolic acid like ellagic acid, gallic acid, chlorogenic acid, caffeic acid, etc. [18]. Apart from its medicinal value, it is abundantly available in the surrounding places of our University and hence was selected in our study. Healthy and fresh *Moringa Oleifera* (Drumstick) leaves were collected in the month of monsoon and cleaned properly by running tap water followed by deionized water. 10 g of washed Drumstick leaves were crushed and kept in a conical flask containing 100 ml of deionized water. The flask was then placed inside a hot air oven at 50 °C for allowing the biomolecules presents in the Drumstick leaves to effuse into the warm water. As a result the colour of the water turns into light yellow. This coloured leaf extract was filtered and then stored in a refrigerator (at 4 °C) for experimental use. Here the precursor material i.e., zinc acetate dihydrate (CAS #: 5970-45-6) and the precipitator i.e., potassium hydroxide (CAS #: 1310-58-3) were purchased from MERCK and were used directly without any further purification. At first, stock solutions of Zinc acetate dihydrate and KOH in deionized water having concentration 10 mM and 30 mM, respectively were prepared. Then from these stock solutions 20 ml of KOH is slowly added into 40 ml of Zinc acetate dihydrate solution kept at $\sim$ 70 °C under continuous stirring. As soon as the addition of KOH solution is complete, 2 ml of previously prepared Drumstick leaf extract was added drop by drop continuing the heated stirring further for next 2 hours. After the stipulated time of reaction, the solution mixture was allowed to cool down at normal temperature and leave it for overnight to precipitate. On the next day the precipitation was collected and washed thrice with double distilled water by centrifuging at 6500 rpm for 5 min. The resulting product was collected from the centrifuge tube and preserved at room temperature for characterization.

For optical and structural studies of the synthesized samples we have used different characterization techniques. For XRD measurements, film of ZnO NPs was deposited on a glass substrate of appropriate size by dropping and drying the liquid sample of ZnO NPs dispersed in water. XRD data was recorded by a Benchtop X-ray diffractometer (Rigaku, Japan, PXRD) operating at 1600 watt and having Cu K_α radiation (1.540 Å). The XRD data were collected from 30° to 70° in 2θ values with scanning rate of 10° per min. UV-Visible spectroscopic studies were performed using a double beam UV-visible spectrophotometer (JASCO V-630). PL emission spectra were obtained by Agilent made Cary Eclipse fluorescence spectrometer. The morphology and chemical composition of the sample were determined through the SEM apparatus (JEOL JSM-IT300HR) furnished by an X-ray energy dispersive spectrometer. Gold coating was made on the sample to increase the surface conductivity before analyzing it by the SEM apparatus. FTIR study was performed using an infrared spectrophotometer (L1600300, Perkin Elmer, UK) operating in the range of 450 cm^{-1} to 4000 cm^{-1} in wavenumber value with a data acquisition rate of 1 cm^{-1} per step.

3. Result and discussion

3.1 X-ray diffraction (XRD) studies

XRD analysis is a basic non-destructive characterization tool providing the details about the crystal structure, phase purity and crystallite size of the synthesized sample. The XRD spectrum of the sample is shown in figure 1 where all the diffraction peaks are marked in the figure. The diffraction peaks appeared at 31.68°, 34.35°, 36.16°, 47.43°, 56.44°, 62.71°, 66.19°, 67.77°, 68.9° in 2θ values corresponding to the diffraction planes (100), (002), (101), (102), (110), (103), (200), (112) and (201), respectively of wurtzite structure of ZnO [21]. The diffraction peaks corresponding to these planes are well agreement with the standard data JCPDS No: 89–1397 [22]. The presence of no other diffraction peak apart from these characteristic peaks in the diffractogram of ZnO suggests high purity of the synthesized sample free from any kind of impurity phases. The average crystallite sizes from the XRD diffraction peaks can be calculated following Debye-Scherrer formula [23]

$$D = \frac{0.94\lambda}{\beta \cos\theta} \tag{1}$$

Here λ represents the wavelength of X-ray radiation and β (in radian) represents the full width at half maxima (FWHM) of the diffraction corresponding to the diffraction angle θ. The average crystallite size as measured from different diffraction peaks were estimated (using equation 1) and

shown in Table 1. From this table it is seen that the average grain sizes of ZnO NPs are found in the range of 45 ± 6 nm. This study suggests that a highly crystalline ZnO NPs has been synthesized.

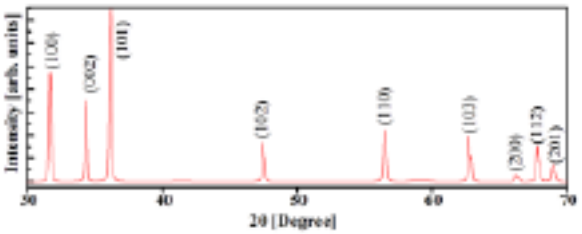

Figure 1. XRD spectra of bio-synthesized ZnO NPs showing diffraction peaks corresponding to various diffraction planes as marked in the figure.

Table 1: Average crystallite sizes of ZnO NPs as measured from XRD peaks corresponding to diffraction planes.

Diffraction Plane (hkl)	2θ (Degree)	FWHM (Degree)	Average crystallite size (nm)
(100)	31.68	0.18	47.94
(002)	34.35	0.17	51.11
(101)	36.16	0.19	45.96
(102)	47.43	0.21	43.17
(110)	56.44	0.24	39.25
(103)	62.71	0.22	44.19

3.2 Scanning electron microscopy (SEM) and energy dispersive X-ray (EDS) spectroscopy

The SEM image and EDS spectrum of ZnO NPs are shown in figure 2(a) and 2(b), respectively. The SEM image shows that the synthesized ZnO NPs form a mesh like structure in the specimen used to study. This mesh like structure of the SEM image may be due to the agglomeration of

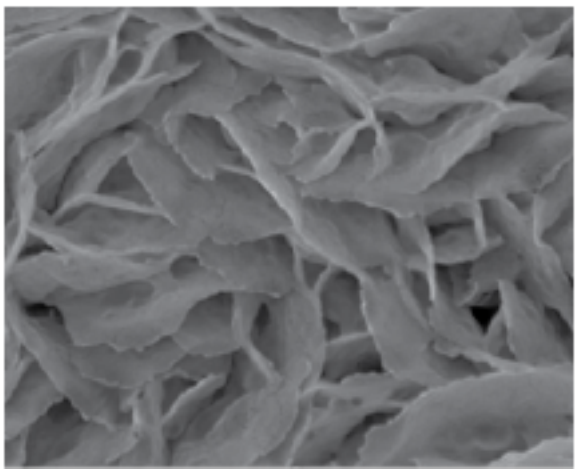

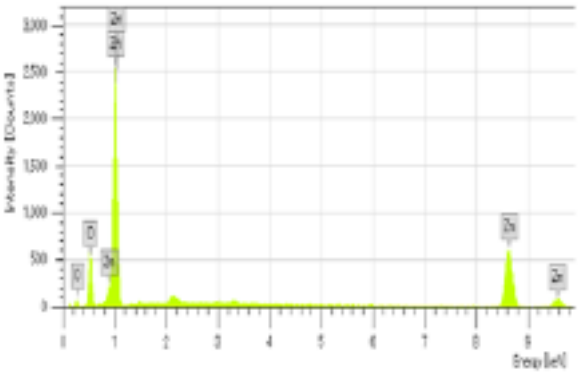

Figure 2. (a) SEM image and (b) EDS spectrum of green synthesized ZnO NPs.

the NPs in the SEM specimen. The strong signals of Zn and O appeared in the EDS spectrum confirm the successful preparation of ZnO NPs. A very weak signal of C in the EDS spectrum indicates the presence of residual biomolecules of the leaf extract within the sample.

3.3 UV-Vis spectroscopy

A comprehensive tool to study the optical properties of nanomaterials is the UV-Visible spectroscopy. Figure 3(a) and 3(b) show the UV-Visible spectrum of the green synthesized ZnO NPs and *Moringa oleifera* aqueous leaf extract, respectively in the wavelength range from 300 nm to 700 nm. The UV-Visible spectrum of *Moringa oleifera* leaf extract shows a monotonically increasing absorbance intensity with decrease in wavelength without showing any structure, while a steep absorption in the UV-Visible spectrum followed by an absorption peak at ~ 352 nm has been appeared. This absorption peak confirms the formation of exciton within ZnO NPs [24, 25]. By absorbing the incident radiation, the electron in the valance band of ZnO NPs reaches at the conduction band leaving behind a hole in the valance

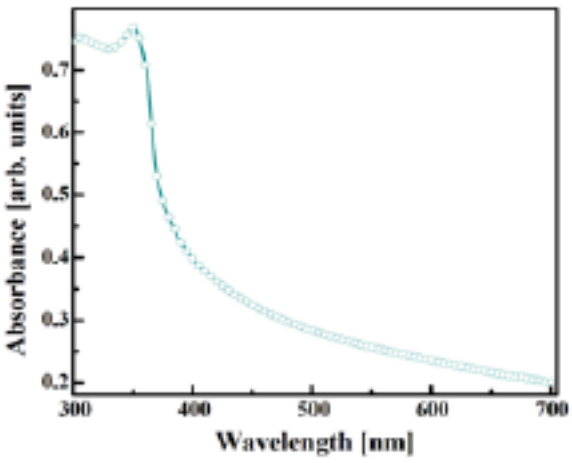

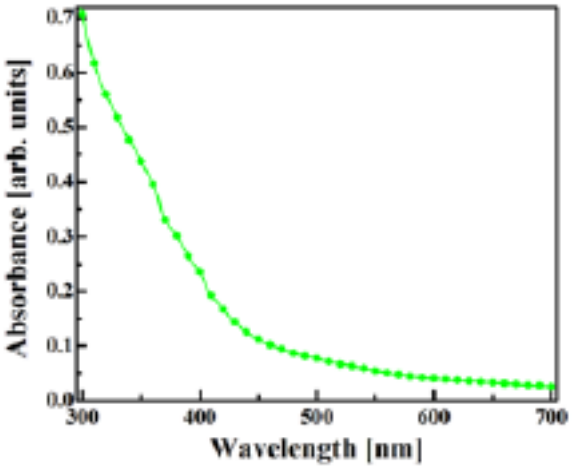

Figure 3. UV-Visible spectrum of (a) green synthesized ZnO NPs and (b) *Moringa oleifera* leaf extract.

band. So, the peak at ∼ 352 nm corresponds to the band gap of ZnO NPs. Because of quantum confinement effect, the UV-Visible absorption peak of the synthesized sample has been shifted towards shorter wavelength side (blueshifted) as compared to its bulk value (377 nm) [26].

3.4 Photoluminescence (PL) spectroscopy

The room temperature PL emission spectrum of the biosynthesized ZnO NPs is shown in figure 4. The spectrum consists of three emission peaks viz. a narrow band in the UV region centered at ∼ 360 nm, a broad emission band in the visible region centered at ∼ 530 nm and a sharp peak centered at ∼ 640 nm which are identified as band edge emission of ZnO, defected mediated emission of ZnO and second harmonic of excitation wavelength, respectively. Here the excitation wavelength used to excite the colloidal sample of ZnO NPs is 320 nm. Being excited by the excitation wavelength the electrons from the valance band reach at the conduction band of ZnO NPs. When these conduction electrons recombine with the holes directly from conduction band to valance band the band edge emission appears which lies in the UV region of the electromagnetic spectrum. These conduction electrons sometime relax at the defect states generated due to oxygen vacancies or zinc interstitial [25] of ZnO and then recombination with holes occurs leading to a broad emission peak in the visible region known as defect mediated emission. The emission peak at 640 nm is an optical phenomenon related to the PL equipment. In our PL set up we always get second harmonic at double value of excitation wavelength.

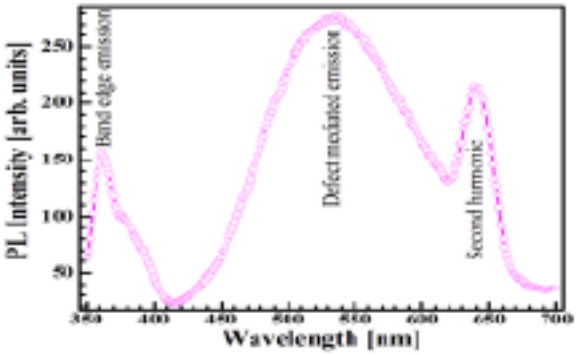

Figure 4. Photoluminescence emission spectrum of green synthesized ZnO NPs showing three emission peaks corresponding to band edge emission, defected mediated of ZnO and second harmonic of excitation wavelength appear from lower to higher wavelength.

3.5 Fourier-transform-infrared (FTIR) spectroscopy

FTIR study was performed to investigate the metal-oxygen bond and contribution of the biocompounds in the synthesis process. Figure 5 shows the FTIR spectrum of the green synthesized ZnO NPs. In the FTIR spectrum the absorption peaks appeared at 460 cm^{-1}, 694 cm^{-1}, 831 cm^{-1}, 1042 cm^{-1}, 1350 cm^{-1}, 1555 cm^{-1}, 2925 cm^{-1} and 3414 cm^{-1}. The intense peak at 460 cm^{-1} refers the stretching of Zn–O bond [27] while all other peaks are due to residual biomolecules present in the ZnO NP's sample. The peak at

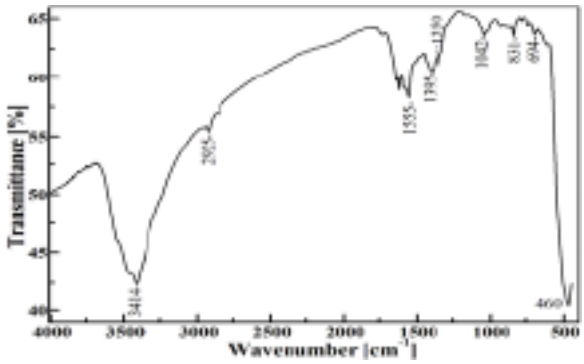

Figure 5. FTIR spectra of green synthesized ZnO NPs.

1042 cm^{-1} is due to the C–N stretching of amine group. The peaks at 1350 cm^{-1} and 1395 cm^{-1} appear due to C–O stretching. The absorption peak at 1555 cm^{-1} refers the presence of amine group (N–H). The peaks at 3414 cm^{-1} and 2925 cm^{-1} are due to the stretching of hydroxyl compounds [28]. FTIR result provides evidences

of the presence of few bioactive compounds which were bound on the surface of ZnO NPs leading to enhance the bioactivity of ZnO. This explains why a weak signal of C in the EDS spectra of the sample has been observed.

4. Conclusion

We have successfully synthesized ZnO NPs at relatively low temperature (~ 70 °C) via green synthesis approach using *Moringa Oleifera* leaves extract as a biogenic reducing and capping agent. This method is very fast, simple, cost-effective and employing of non-toxic chemicals and hence it is considered as eco-friendly approach. The prepared sample was highly crystalline with wurtzite crystal structure as revealed from XRD study. The obtained crystals of ZnO NPs are free from any type of impurity and hence are pure. The average crystallite sizes of the NPs are estimated as 45 ± 6 nm. From the EDS spectrum the chemical composition of the NPs sample has been verified. The steep absorption peak at ~ 352 nm in the UV-Visible spectrum authenticates the formation of ZnO NPs. Due to the quantum confinement effect, the optical absorption peak position of the sample is seen to be blue shifted in comparison to the bulk value of ZnO. This shift is due to the enhancement of band gap energy of ZnO due to its nano sized. The narrow PL emission band in the UV region centered at ~ 360 nm confirms the formation of green synthesized ZnO NPs. The formation of Zn–O bond was confirmed by the intense peak appeared at ~ 460 cm^{-1} in the FTIR spectrum of the sample.

References

[1] K Kaviyarasu, C Maria Magdalane, K Kanimozhi, et al. Elucidation of photocatalysis, photoluminescence and antibacterial studies of ZnO thinfilms by spin coating method, J Photochem Photobiol B Biol., 173, 466–475 (2017).

[2] Q F Zhang, C S Dandeneau, X Y Zhou, et al. ZnO nanostructures for dye-sensitized solar cells, Adv Mater., 21, 4087–4108 (2009).

[3] A M Holmes, Z Song, H R Moghimi, et al., Relative penetration of zinc oxide and zinc ions into human skin after application of different zinc oxide formulations, ACS Nano., 10, 1810–1819 (2016).

[4] Z Jia, R D K Misra, Tunable ZnO quantum dots for bioimaging: synthesis and photoluminiscence, Mater Technol, 28, 221–227 (2013).

[5] T Ghosh, A Chattopadhyay, S Pramanik, S Mukherjee, S Das, A C Mandal, P K Kuiri, Bio-synthesis of ZnO nanoparticles and their in-situ coating on cotton fabric using Azadirachta Indica leaf extract for enhanced antibacterial activity, Mater. Technol, (2021), https://doi.org/10.1080/10667857.2021.1978755

[6] P K Giri, S Bhattacharyya, D K Shing, R Kesavamoorthy, B K Panigrahi, K G M Nair, Correlation between microstructure and optical properties of ZnO nanoparticles synthesized by ball milling, J. Appl. Phys., 102, 093515 (2007).

[7] P. K. Kuiri and D. P. Mahapatra, Effects of annealing atmosphere on ZnO-ions-implanted silica glass: synthesis of Zn and ZnO nanoparticles, J. Phys. D: Appl. Phys., 43, 395404 (2010).

[8] M Ranjbar, M A Taher, A Sam, Solvent-free synthesisof Zno nanoparticles by a simple thermal decomposition method, J Clust Sci., 25, 1657–1664 (2014).

[9] K Subalakshmi, J Senthilselvan, K A Kumar, et al, Solvothermal synthesis of hexagonal pyramidal and bifrustum shaped ZnO nanocrystals: natural betacyanindye and organic Eosin Y dye sensitized DSSCefficiency, electron transport, recombination dynamicsand solar photodegradation investigations, J Mater SciMater Electron., 28, 15565–15595 (2017).

[10] A A Ismail, A El-Midany, E A Abdel-Aal, et al. Application of statistical design to optimize the preparation of ZnO nanoparticles via hydrothermal technique, Mater Lett., 59, 1924–1928 (2005).

[11] M M Ba-Abbad, A A H Kadhum, A B Mohamad, et al. The effect of process parameters on the size of ZnO nanoparticles synthesized via the sol–gel technique. J Alloys Compd., 550, 63–70 (2013).

[12] S. Pramanik, T. Ghosh, M. Ghosh, S. C. De, P. K. Kuiri, Synthesis and time dependent growth of ZnO nanoparticles using solution route, and the defect-free luminescence, Adv. Sci. Eng. Med., 9, 414–419 (2017).

[13] S. Pramanik, T. Ghosh, M. Ghosh, S. C. De, P. K. Kuiri, Quenching of Blue–Green Luminescence of ZnO Nanoparticles Obtained by Solution Route with Different Precursor Concentration, J. Nanoelectron. Optoelectron., 13, 428–433 (2018).

[14] F Sheikh, Q K Panhwar, A Balouch, S Ali, W A Panhwar, F Sheikh, Synthesis of zinc oxide nanoparticles and their functionalisation with chrysin: Exploration and its application, Int. J. Environ. Anal. Chem. 2020, https://doi.org/10.1080/03067319.2020.1742889

[15] T. Ghosh, A. Chattopadhyay, A. C. Mandal, S. Pramanik, P. K. Kuiri, Optical, structural, and antibacterial properties of biosynthesized Ag nanoparticles at room temperature using Azadirachta indica leaf extract, *Chin. J. Phys.*, 68, 835–848 (2020).

[16] T. Ghosh, A. Chattopadhyay, A. C. Mandal, S. Pramanik, S. Mukherjee, P. K. Kuiri,

Spectroscopic, microscopic and antibacterial studies of green synthesized Ag nanoparticles at room temperature using Psidium guajava leaf extract, *Korean J. Chem. Eng.* (2021). https://doi.org/10.1007/s11814-021-0918-x

[17] H Agarwal, S V Kumar, S Rajeshkumar, A review on green synthesis of zinc oxide nanoparticles—An eco-friendly approach, Resource-Efficient Technologies, 3, 406–413 (2017).

[18] N Matinise, X G Fuku, K Kaviyarasu, N Mayedwa, M Maaza, ZnO nanoparticles via Moringa oleifera green synthesis: Physical properties & mechanism of formation, Applied Surface Science, 406, 339–347 (2017).

[19] S Pal, S Mondal, J Maity, R Mukherjee, Synthesis and Characterization of ZnO Nanoparticles using Moringa Oleifera Leaf Extract: Investigation of Photocatalytic and Antibacterial Activity, Int. J. Nanosci. Nanotechnol., 14, 111–119 (2018).

[20] F Alhakmani, S Kumar, SAKhan, Estimation of total phenolic content, in-vitro antioxidant and anti-inflammatory activity of flowers of Moringa oleifera, Asian Pac J Trop Biomed, 3, 623–627 (2013).

[21] S Mukherjee, S Pramanik, S Das, S Chakraborty, R Nath, P K Kuiri, Structural, optical, and electrical properties of Zn1-xAlxO nanoparticles near the Al solubility limit, J Alloys Compd, 814, 152015 (2020).

[22] S. Nagarajan, K. A. Kuppusamy, Extracellular synthesis of zinc oxide nanoparticle using seaweeds of gulf of Mannar, India, J Nanobiotechnol, 11, 39 (2013).

[23] S Pramanik, S Mondal, A C Mandal, S Mukherjee, S Das, T Ghosh, R Nath, M Ghosh, P K Kuiri, Role of oxygen vacancies on the green photoluminescence of microwave-assisted grown ZnO nanorods, J. Alloys Compd., 849, 156684 (2020).

[24] S Talam, S R Karumuri, N Gunnam, Synthesis, Characterization, and Spectroscopic Properties of ZnO Nanoparticles, International Scholarly Research Notices, 2012, 372505, 2012.

[25] P. K. Kuiri, S. Pramanik, Large enhancement of UV luminescence emission of ZnO nanoparticles by coupling excitons with Ag surface plasmons, J. Appl. Phys., 123, 154302 (2018).

[26] M. Ghosh and A. K. Raychaudhuri, Shape transition in ZnO nanostructures and its effect on blue-green photoluminescence, Nanotechnology 19, 445704 (2008).

[27] N Jayaprakash, R Suresh, S Rajalakshmi, S Raja, E Sundaravadivel, M Gayathri, M Sridharan, One-step synthesis, characterisation, photocatalytic and bio-medical applications of ZnO nanoplates, Mater. Technol., 35, 112–124 (2020).

[28] N Jayarambabu, B S Kumari, K. V Rao, Y T Prabhu, Germination and Growth Characteristics of Mungbean Seeds (Vigna radiata L.) affected by Synthesized Zinc Oxide Nanoparticles, International Journal of Current Engineering and Technology, 4, 3411–3416 (2014).